THE JOURNAL OF BIOLOGICAL CHEMISTRY
Vol. 276, No. 49, Issue of December 7, pp. 46196–46203, 2001

Printed in U.S.A.

The Polyphosphate Bodies of *Chlamydomonas reinhardtii* Possess a Proton-pumping Pyrophosphatase and Are Similar to Acidocalcisomes*

Received for publication, June 7, 2001, and in revised form, September 27, 2001
Published, JBC Papers in Press, September 28, 2001, DOI 10.1074/jbc.M105268200

Felix A. Ruiz‡, Norma Marchesini‡, Manfredo Seufferheld‡§, Govindjee§, and Roberto Docampo‡¶

From the ‡Laboratory of Molecular Parasitology, Department of Pathobiology, and the §Department of Plant Biology, University of Illinois at Urbana-Champaign, Urbana, Illinois 61802

Acidocalcisomes are acidic calcium storage compartments described initially in trypanosomatid and apicomplexan parasites. In this work, we describe organelles with properties similar to acidocalcisomes in the green alga *Chlamydomonas reinhardtii*. Nigericin and NH_4Cl released $^{45}Ca^{2+}$ from preloaded permeabilized cells, suggesting the incorporation of a significant amount of this cation into an acidic compartment. X-ray microanalysis of the electron-dense vacuoles or polyphosphate bodies of *C. reinhardtii* showed large amounts of phosphorus, magnesium, calcium, and zinc. Immunofluorescence microscopy, using antisera raised against a peptide sequence of the vacuolar type proton pyrophosphatase (H^+-PPase) of *Arabidopsis thaliana* which is conserved in the *C. reinhardtii* enzyme, indicated localization in the plasma membrane, in intracellular vacuoles, and the contractile vacuole where it colocalized with the vacuolar proton ATPase (V-H^+-ATPase). Purification of the electron-dense vacuoles using iodixanol density gradients indicated a preferential localization of the H^+-PPase and the V-H^+-ATPase activities in addition to high concentrations of PP_i and short and long chain polyphosphate, but lack of markers for mitochondria and chloroplasts. In isolated electron-dense vacuoles, PP_i-driven proton translocation was stimulated by potassium ions and inhibited by the PP_i analog aminomethylenediphosphonate. Potassium fluoride, imidodiphosphate, *N*,*N*′-dicyclohexylcarbodiimide, and *N*-ethylmaleimide also inhibited PP_i hydrolysis in the isolated organelles in a dose-dependent manner. These results indicate that the electron-dense vacuoles of *C. reinhardtii* are very similar to acidocalcisomes with regard to their chemical composition and the presence of proton pumps. Polyphosphate was also localized to the contractile vacuole by 4′,6-diamidino-2-phenylindole staining, suggesting, with the immunochemical data, a link between these organelles and the acidocalcisomes.

Intracellular granules of microorganisms that stain with basic dyes have been referred to as volutin or metachromatic granules (1). It is generally agreed that volutin granules contain polyphosphate, a linear polymer of many tens or hundreds of orthophosphate (P_i) residues linked by high energy phosphoanhydride bonds (2, 3). This conclusion initially derived from the correlation of the polyphosphate content of yeast cells with the number and size of the volutin granules (2). The presence of volutin granules or polyphosphate bodies has been described in bacteria, algae, yeast, and protozoa (3).

In algae, polyphosphate bodies are characterized by their high electron density when observed by electron microscopy (4). Recent isolation of these electron-dense bodies from the cell wall-deficient biflagellate green alga *Chlamydomonas reinhardtii* allowed the demonstration of the presence of pyrophosphate (PP_i)[1] and polyphosphate, as measured by ^{31}P NMR, and phosphorus, magnesium, and calcium, as detected by x-ray microanalysis (5).

In recent years electron-dense vacuoles similar to the polyphosphate bodies and containing high concentrations of PP_i, polyphosphate, calcium, magnesium, and other elements have been found in trypanosomatids and apicomplexan parasites and named acidocalcisomes (6). In addition, these organelles were shown to contain proton and calcium pumps and several exchangers in their limiting membrane (6). The presence of such transporters has not been investigated in the polyphosphate bodies of other microorganisms, and it is not known whether they represent the same organelle.

One of the pumps present in acidocalcisomes is the vacuolar type H^+-translocating pyrophosphatase (H^+-PPase). H^+-PPases have also been described in plants, algae, and bacteria (7, 8). A potassium-stimulated pyrophosphatase activity was detected by measurement of PP_i hydrolysis in microsomal fractions of *C. reinhardtii* (9). Because a protein of similar molecular weight to a plant H^+-PPase was recognized by polyclonal antibodies raised against the enzyme from the tonoplast of mung bean hypocotyl, the presence of an H^+-PPase was postulated (9). This protein was localized in the plasma membrane, contractile vacuole, and unidentified "intermediate size vesicles" (9).

To demonstrate that acidocalcisomes and polyphosphate bodies are representatives of the same organelle we investigated whether the morphologically and chemically well characterized polyphosphate bodies of *C. reinhardtii* also possessed enzymatic activities in their limiting membranes. We report the isolation of these polyphosphate bodies, which were identified by their elemental and polyphosphate content. The or-

* This work was supported in part by National Institutes of Health Grant AI-23259 (to R. D.) and National Science Foundation Photosynthesis Training Grant DBI 96-02240 (to G.). The costs of publication of this article were defrayed in part by the payment of page charges. This article must therefore be hereby marked "*advertisement*" in accordance with 18 U.S.C. Section 1734 solely to indicate this fact.

¶ To whom correspondence should be addressed: Laboratory of Molecular Parasitology, Dept. of Pathobiology, College of Veterinary Medicine, University of Illinois at Urbana-Champaign, 2001 South Lincoln Ave., Urbana, IL 61802. Tel.: 217-333-3845; Fax: 217-244-7421; E-mail: rodoc@uiuc.edu.

[1] The abbreviations used are: PP_i, pyrophosphate; H^+-PPase, proton pyrophosphatase; V-H^+-ATPase, vacuolar proton ATPase; PBS, phosphate-buffered saline; AMDP, aminomethylenediphosphonate; DAPI, 4′,6-diamidino-2-phenylindole; DCCD, *N*,*N*′-dicyclohexylcarbodiimide.

ganelles were shown to possess vacuolar proton ATPase (V-H^+-ATPase) and H^+-PPase activities. The H^+-PPase was shown to possess similar characteristics to the plant, bacterial, and acidocalcisomal H^+-PPase. An unexpected finding was the colocalization of these proton pumps, as well as polyphosphate, in the contractile vacuoles, suggesting a link between these two cellular organelles. Our results imply that the phylogenetic distribution of acidocalcisomes is much wider than proposed previously.

EXPERIMENTAL PROCEDURES

Cell Cultures—C. reinhardtii cell wall(−) wild type strain, isolated after ARG7 insertional mutagenesis of the parental strain CC425 (10), was provided by Dr. K. Niyogi (University of California, Berkeley). Cells were grown photoheterotrophically in Tris acetate phosphate (TAP) medium (11) with agitation. The temperature was maintained at 25 °C, and the light intensity was 100 μmol of photons/$m^2 \times s^{-1}$, provided by 40-W cool white fluorescent lamps. Cells were harvested at the late exponential growth phase.

Chemicals—ATP, Dulbecco's PBS, digitonin, and reagents for marker enzyme assays were purchased from Sigma. Silicon carbide (400 mesh) was bought from Aldrich. Iodixanol (40% solution (OptiPrep, Nycomed)) was obtained from Life Technologies, Inc. Monoclonal antibody N-2 against the 110-kDa accessory protein of the *Dictyostelium discoideum* V-H^+-ATPase (12) was purchased from the Monoclonal Antibody Center of the University of Hawaii. Polyclonal antibodies raised against a keyhole limpet hemocyanin-conjugated synthetic peptide corresponding to the hydrophilic loop XII (antibody PAB_{HK} or 326) of plant H^+-PPase (13) and aminomethylenediphosphonate (AMDP) (14) were kindly provided by Prof. Philip Rea, University of Pennsylvania (Philadelphia). Molecular weight markers and Coomassie Blue protein assay reagent were from Bio-Rad. The EnzChek phosphate assay kit was from Molecular Probes (Eugene, OR). *Escherichia coli* strain CA38 pTrcPPX1 was kindly provided by Prof. Arthur Kornberg, Stanford University School of Medicine (Stanford, CA). All other reagents were of analytical grade.

Release of $^{45}Ca^{2+}$ from Permeabilized Cells—$^{45}Ca^{2+}$ release was measured as described previously (5) with minor modifications. Cells (1×10^7) were washed twice with Dulbecco's PBS and incubated in 1 ml of 1 mM KCl, 1 mM $MgCl_2$, 0.1 mM K_2HPO_4, 0.1 mM $CaCl_2$, and 10 mM Hepes, pH 7.2 (buffer C), with 0.1 mCi/ml of $^{45}CaCl_2$ for 3 h. After washing the cells twice by centrifugation with PBS, they were suspended in 3 ml of buffer C plus 20 mM EGTA, and 20 μM digitonin was added. These permeabilized cells were incubated in the presence or absence of 5 μM nigericin or 20 mM NH_4Cl at 37 °C for different periods of time. Aliquots were taken and filtered through Whatman GT glass microfiber filters and washed three times with 3 ml of ice-cold 1 mM EGTA in 10 mM Hepes, pH 7.2, and the radioactivity of the filters was measured by scintillation counting.

Isolation of Electron-dense Vacuoles—Cells were collected by centrifugation and washed twice in Dulbecco's PBS and once in lysis buffer (125 mM sucrose, 50 mM KCl, 4 mM $MgCl_2$, 0.5 mM EDTA, 20 mM K-Hepes, 5 mM dithiothreitol, 0.1 mM 4-(2-aminoethyl)benzenesulfonyl fluoride, 10 μM pepstatin, 10 μM leupeptin, 10 μM *trans*-epoxysuccinyl-L-leucylamido-(4-guanidino) butane, and 10 μM N^{α}-tosyl-L-lysine chloromethyl ketone, pH 7.2). The cell pellet was mixed with 1.5 × wet weight silicon carbide and lysed by grinding with a pestle and mortar for at least 4 min. Lysis was monitored by optical microscopy. The lysate was clarified first by centrifugation at 144 × *g* for 5 min then at 325 × *g* for 10 min. The second pellet was washed under the same conditions, and the supernatant fractions were combined and centrifuged for 30 min at 10,500 × *g*. The pellet was resuspended in 4 ml of lysis buffer with the aid of a 22-gauge needle and applied to a discontinuous gradient of iodixanol, with 4-ml steps of 24, 28, 34, 37, and 40% iodixanol, diluted in lysis buffer (15). The gradient was centrifuged at 50,000 × *g* in a Beckman SW28 rotor for 60 min. The electron-dense vacuole fraction pelleted on the bottom of the tube and was resuspended in lysis buffer. Gradient fractions were assayed as described previously for cytochrome *c* oxidase (16) (mitochondrial marker), glyceraldehyde-3-phosphate dehydrogenase (17) (chloroplast marker), 1 μM bafilomycin A_1-sensitive vacuolar H^+-ATPase (15) (contractile vacuole marker; Refs. 12, 18, and 19), and vacuolar pyrophosphatase (15), short chain and long chain polyphosphate (20, 21), and PP_i (20). The construction of normalized density distribution histograms was carried out as described before (22).

Extraction and Analysis of Long and Short Chain Polyphosphate and PP_i—Cells (1×10^7–1×10^8) were washed once with Dulbecco's PBS and treated to extract either long chain or short chain polyphosphate. Different samples were used in each case. Long chain polyphosphate extraction was performed as described by Ault-Riché *et al.* (21). For PP_i and short chain polyphosphate extraction, the cell pellet was resuspended in ice-cold 0.5 M $HClO_4$ (2 ml/g of wet weight of cells). After 30 min of incubation on ice, the extracts were centrifuged at 14,000 × *g* for 30 s. The supernatants were neutralized by the addition of 0.72 M KOH and 0.6 M $KHCO_3$. Precipitated $KClO_4$ was removed by centrifugation at 14,000 × *g* for 30 s, and the extracted supernatant was used for polyphosphate and PP_i determination. Polyphosphate levels were determined from the amount of P_i released upon treatment with an excess of purified recombinant exopolyphophatase from *Saccharomyces cerevisiae* as described previously (20). PP_i levels were determined from the amount of P_i released upon treatment with inorganic pyrophosphatase (Sigma, final activity 10 units/ml) as described previously (20).

Characterization of Pyrophosphatase Activity—Pyrophosphatase was assayed by measuring released phosphate using the EnzChek phosphate assay as described before (15, 23). Reaction mixtures contained 130 mM KCl, 10 mM Hepes, pH 7.2, 2 mM $MgSO_4$, 50 μM EGTA, 0.1 mM 2-amino-6-mercapto-7-methylpurine ribonucleoside, 0.4 unit/ml purine nucleoside phosphorylase, 0.2–0.4 mg of electron-dense vacuole fraction, and PP_i as indicated in a total volume of 0.1 ml. Activity was recorded at 360 nm and 30 °C in a PowerWave 340i plate reader (Bio-tek Instruments, Minnoski, VT).

H^+ Transport—PP_i-driven H^+ uptake into electron-dense vacuoles was assayed using acridine orange as described before (23), except that the standard buffer used was 120 mM KCl, 2 mM $MgCl_2$, 50 mM K-Hepes, 50 μM EGTA, pH 7.2.

Immunoblot Methods—15-μl aliquots of the *Chlamydomonas* subcellular fractions were mixed with 15 μl of electrophoresis buffer (125 mM Tris/HCl, pH 7, 10% (w/v) β-mercaptoethanol, 20% (v/v) glycerol, 4% (w/v) bromphenol blue) and boiled for 5 min prior to application to 10% SDS-polyacrylamide gels. Electrophoresed proteins were transferred to nitrocellulose using a Bio-Rad transblot apparatus. Membranes were blocked in 5% non-fat dry milk in PBS and kept overnight at 4 °C. A 1:10,000 dilution of antiserum 326 against H^+-PPase in blocking buffer was applied to blots at room temperature for 60 min. The nitrocellulose was washed three times for 20 min each with PBS (containing 0.1% (v/v) Tween 20), before the addition of a 1:20,000 dilution of goat anti-rabbit IgG in blocking buffer for 30 min. Immunoblots were visualized on radiographic film (Kodak) using the ECL detection kit (Amersham Pharmacia Biotech).

Fluorescence Microscopy—For 4′,6-diamidino-2-phenylindole (DAPI) staining, cells (5×10^7) obtained as described above were washed twice with Dulbecco's PBS and fixed for 30 min with 2% glutaraldehyde in Dulbecco's PBS. The cells were centrifuged at 14,000 × *g* for 1 min, and the pellet was resuspended in 0.5 ml of Dulbecco's PBS. 45 μl of this suspension was incubated at room temperature with 10 μg of DAPI and 40 μM digitonin. After 10 min, the samples were mounted on a slide and observed with an Olympus laser scanning confocal microscope using optical sections of 0.1 μm and an argon laser for detection of polyphosphate (20).

For immunofluorescence experiments cells fixed with 4% formaldehyde (freshly prepared) were allowed to adhere to poly-L-lysine-coated coverslips, permeabilized with 0.3% Triton X-100 and 3% albumin for 5 min, and prepared for immunofluorescence with a 1:100 dilution of antibody PAB_{HK} (326) or a 1:100 dilution of the monoclonal antibody N-2 and a rhodamine-coupled goat anti-rabbit immunoglobulin G (IgG) or fluorescein isothiocyanate-coupled goat anti-mouse IgG secondary antibody (1:150), respectively. Control preparations were incubated with preimmune serum or without the primary antibody. Immunofluorescence images were obtained with the laser scanning confocal microscope using krypton and argon lasers for detection of the fluorescent dyes.

Electron Microscopy and X-ray Microanalysis—For imaging whole cells and electron-dense vacuole fractions the preparations were washed in 0.25 M sucrose, and a 5-μl sample was placed on a Formvar-coated 200-mesh copper grid, allowed to adhere for 10 min at room temperature, blotted dry, and observed directly with a Hitachi 600 transmission electron microscope operating at 100 kV (15, 23). Energy-dispersive x-ray analysis was done at the Electron Microscopy Center, Southern Illinois University (Carbondale, IL). Specimen grids were examined in a Hitachi H-7100FA transmission electron microscope at an accelerating voltage of 50 kV. Fine probe sizes were adjusted to cover the electron-dense vacuoles (or a similar area of the background), and x-rays were collected for 100 s by utilizing a thin window (Norvar)

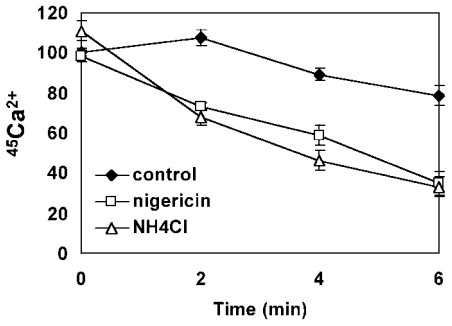

FIG. 1. **Effect of NH_4Cl and nigericin on $^{45}Ca^{2+}$ release from *Chlamydomonas* permeabilized cells.** $^{45}Ca^{2+}$-loaded cells were permeabilized with 20 μM digitonin and exposed to 20 mM NH_4Cl (*open triangles*), 5 μM nigericin (*open squares*), or buffer alone as control (*closed diamonds*). Other experimental details are given under "Experimental Procedures." The chart shows mean ^{45}Ca activity remaining in the cells ± S.E. of at least three experiments.

detector. Analysis was performed by using a Noran Voyager III analyzer with a standardless analysis identification program.

RESULTS

Presence of an Acidic Calcium Pool in C. reinhardtii—The acidocalcisome has been defined as a calcium-containing acidic compartment (6). To investigate whether Ca^{2+} was present in an acidic compartment of *C. reinhardtii,* we loaded the cells with $^{45}Ca^{2+}$, permeabilized them with digitonin, and measured the release of Ca^{2+} in the presence or absence of agents known to alkalinize acidic compartments, such as the K^+/H^+ ionophore nigericin and the weak base NH_4Cl (6). Addition of these compounds resulted in release of more than 60% of the incorporated ^{45}Ca over a period of 6 min (Fig. 1), whereas a slower ^{45}Ca release was observed in the absence of nigericin or NH_4Cl. The results suggested the presence of a significant amount of Ca^{2+} incorporated into an acidic intracellular compartment of *C. reinhardtii*.

Elemental Analysis and Isolation of Electron-dense Vacuoles of Chlamydomonas—Acidocalcisomes are recognized as vacuoles of high electron density when they are observed in transmission electron micrographs of intact cells (6). Similar vacuoles of varying sizes and high electron density were seen when whole *Chlamydomonas* cells were observed by transmission electron microscopy without fixation and staining (Fig. 2*A*). About 30–40 vacuoles were observed in each cell with an average diameter of about 200 nm. X-ray microanalysis was performed on these dense organelles to investigate their elemental composition (Fig. 2*B*). The spectra generated showed that they contained phosphorus, calcium, and magnesium. Zinc was present in 3 of 10 spectra obtained. In the representative spectrum shown (Fig. 2*B*), peaks for phosphorus were about 3-fold greater than peaks for calcium, which were about 2-fold greater than peaks for magnesium. Peaks for calcium, phosphorus, magnesium, and zinc were not present in spectra taken from the background (Fig. 2*C*). The copper peaks were generated from the copper grid and were not present when nickel grids were used (not shown).

To purify the electron-dense vacuoles of *C. reinhardtii* and investigate whether they were similar to acidocalcisomes from trypanosomatid parasites we adapted the purification procedure used for the isolation of acidocalcisomes from *Trypanosoma cruzi* (15). The utility of the method was assessed by assaying marker enzymes (Fig. 3). Pyrophosphatase, the most conspicuous marker of acidocalcisomes (15), was assessed as the PP_i hydrolytic activity sensitive to the specific H^+-PPase inhibitor AMDP (14). Its yield in fractions 23–24 (the densest fractions, containing the electron-dense vacuoles, see below)

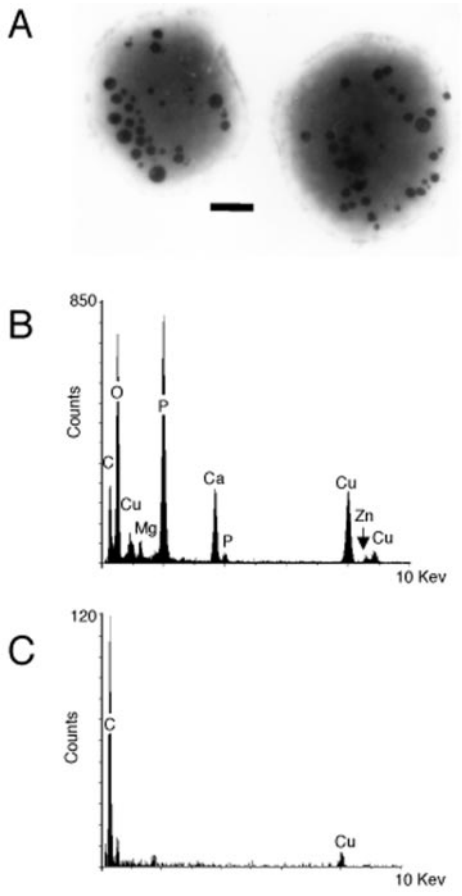

FIG. 2. **Electron microscopy and x-ray microanalysis of whole *Chlamydomonas* cells.** *Panel A*, visualization of electron-dense vacuoles in whole unfixed cells allowed to adhere to a Formvar and carbon-coated grid and then observed in the transmission electron microscope. A large number of dense vacuoles of varying sizes can be seen. *Bar*, 1 μm. *Panel B*, x-ray microanalysis spectrum of dense organelles in whole cells. *Panel C*, x-ray microanalysis spectrum of background.

was 17%, whereas the yield of protein was only 0.15%, a 113-fold purification. This may actually be a large underestimate of the degree of purification of the electron-dense vacuoles because an H^+-PPase was also postulated to be located on the cell surface and contractile vacuole of *Chlamydomonas* (9). Mitochondria (marked by cytochrome *c* oxidase; Ref. 16) and chloroplasts (marked by glyceraldehyde 3-phosphate dehydrogenase; Ref. 17) were not enriched in the electron-dense vacuole fractions. The electron-dense vacuole fractions (fractions 23 and 24) contained more than 35% of the total amounts of PP_i, and short and long chain polyphosphate, and about 25% of the total bafilomycin A_1-sensitive ATPase activity. Taking into account the low protein concentration of these fractions (0.15%) this also represents a more than 100-fold purification of these molecules or activities. The electron-dense vacuole fractions were therefore enriched at least 100-fold more than other cell compartments by this technique. Electron microscopy of fractions 23 and 24, by observation of air-dried samples (Fig. 4*A*), had the same appearance as the acidocalcisomal fractions from *T. cruzi* (23). As occurs with the *T. cruzi* organelles (24), when they were submitted to the electron beam changes in their internal structure led to the appearance of a sponge-like structure (Fig. 4*A*, *inset*). The results of x-ray microanalysis of the organelles (Fig. 4*B*) were similar to those of whole cells except that more magnesium and potassium and less calcium and zinc were detected relative to the phosphorus peak, probably because of ionic changes occurring during the fractionation procedure.

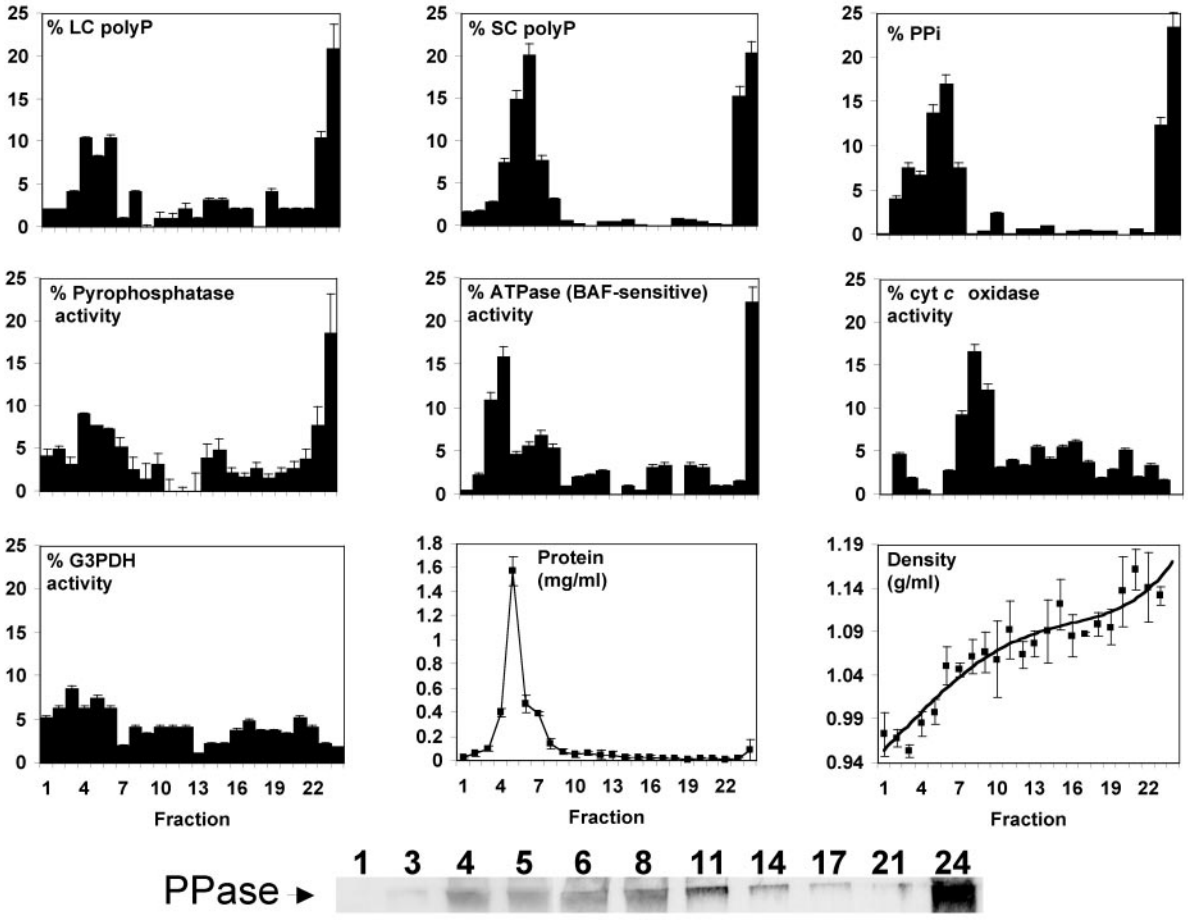

FIG. 3. **Distribution of different markers from *Chlamydomonas* on iodixanol gradients.** PPase activity, PP_i, bafilomycin A_1 (*BAF*)-sensitive ATPase activity, and short and long chain polyphosphate (*SC polyP* and *LC polyP*, respectively) are concentrated in a distinct dense fraction. This distribution was compared with that of established organelle markers, glyceraldehyde-3-phosphate dehydrogenase (*G3PDH*) (chloroplasts) and cytochrome *c* oxidase (*cyt c oxidase*) (mitochondria). Protein distribution in the different fractions is indicated by *closed squares* in the *central lower panel*. *Lower panel*, immunoblots (antibody 326) of iodixanol fractions (*1–24*, corresponding to fractions in other *panels*).

H^+-PPase in Electron-dense Vacuoles of C. reinhardtii—When acridine orange was added to electron-dense vacuole fractions of *C. reinhardtii* some dye was accumulated and retained in the absence of added energy sources (Fig. 5*A*). Once a steady state of acridine orange accumulation was reached, the addition of 0.1 mM PP_i led to further dye uptake, indicating increasing vesicular acidity. Acridine orange accumulation was inhibited by AMDP (Fig. 5*B*, compare *trace b* with *trace a*). 10 μM AMDP released acridine orange when added after acidification had started (Fig. 5, *A* and *B*, *trace a*). The vesicle pH was neutralized, and acridine orange release also occurred after addition of 10 mM NH_4Cl (Fig. 5*A*).

Pyrophosphatase was also assayed in electron-dense vacuole preparations by P_i detection (23). Control pyrophosphatase activity was 0.54 ± 0.025 μmol of PP_i consumed/min/mg of protein (means ± S.E. of results from 12 separate experiments) and was inhibited by 30 μM AMDP by 80 ± 5.3% (average ± S.E. of 10 experiments). The effects of monovalent cations on AMDP-inhibitable PP_i hydrolysis are shown in Table I. Replacing 130 mM KCl with 250 mM sucrose in the buffer resulted in lower pyrophosphatase activity that was reduced further by replacement of 130 mM KCl with 130 mM NaCl or 65 mM NaCl, 125 mM sucrose. Use of a buffer containing equimolar concentrations of NaCl (65 mM) and KCl (65 mM) resulted in lower PP_i hydrolysis than in the presence of 130 mM KCl or 65 mM KCl, 125 mM sucrose. These results suggest that K^+ was necessary for this activity, whereas Na^+ was inhibitory.

The dependence of the initial rate of PP_i hydrolysis on PP_i concentration in *C. reinhardtii* electron-dense vacuoles is shown in Fig. 6*A*. Activity was maximal at about 50 μM PP_i. Standard procedures were used to determine kinetic parameters. A K_m value of 12.3 ± 5.3 μM and a V_{max} of 0.54 ± 0.04 μmol of P_i/min/mg of protein were calculated. Fig. 6*B* shows the effect of medium pH on the initial rate of PP_i hydrolysis in *C. reinhardtii* electron-dense vacuoles. Activity was optimal in the pH range 6.8–7.2.

Inhibition of H^+-PPase Activity—PP_i hydrolysis of the electron-dense vacuole fraction was inhibited, in a dose-dependent manner, by AMDP (Fig. 7*A*). Some residual PP_i hydrolysis activity could be detected even at 30 μM AMDP. There may be an AMDP-insensitive pyrophosphatase activity present in the fraction as well as the H^+-PPase (see also Table I). The activity was also inhibited, in a dose-dependent manner, by the PP_i analog imidodiphosphate (IDP) (Fig. 7*B*). Fig. 8 shows that potassium fluoride greatly inhibited this activity in a dose-dependent manner (Fig. 8*A*), whereas the thiol reagent *N*-ethylmaleimide was a weak inhibitor even at a concentration of 100 μM (Fig. 8*B*). DCCD, an agent known to inhibit other H^+-PPases (25) was also effective in inhibiting the *C. reinhardtii* pyrophosphatase activity in a dose-dependent manner (Fig. 8*C*).

Immunological Evidence of Localization of the H^+-PPase and Its Colocalization with the V-H^+-ATPase—We investigated the localization of the H^+-PPase in *C. reinhardtii* by immunocytochemistry using an antibody against a conserved peptide of *Arabidopsis thaliana* H^+-PPase. This antibody recognizes a

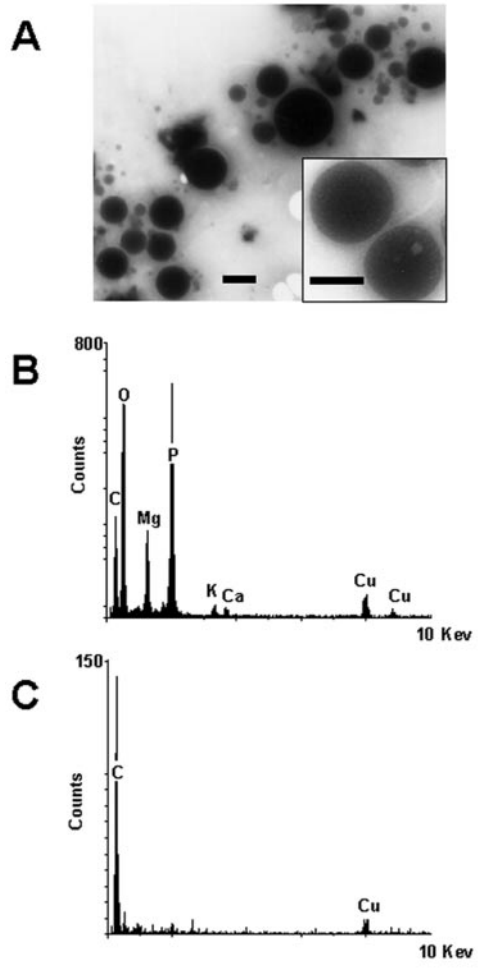

FIG. 4. **Electron microscopy and x-ray microanalysis of the dense fraction containing PPase activity.** *Panel A*, direct observation of iodixanol fraction 24. *Scale bar*, 1 μm. The *inset* in *panel A* shows, at higher magnification, the sponge-like structure of the electron-dense vacuoles after submission to the electron beam. *Panel B*, x-ray microanalysis spectrum of electron-dense vacuoles in fraction 24. *Panel C*, x-ray microanalysis spectrum of background of fraction 24 preparations.

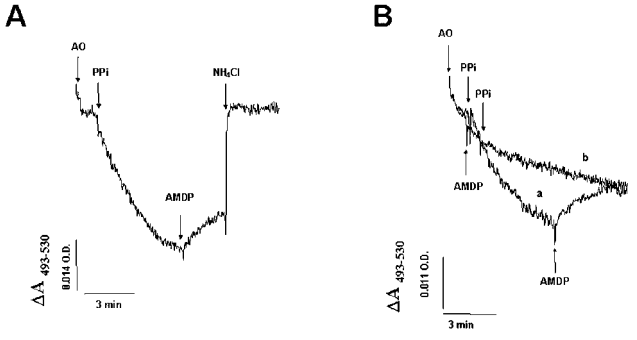

FIG. 5. **PP_i-driven proton transport in *Chlamydomonas* electron-dense vacuoles.** Isolated electron-dense vacuoles (63 μg protein/ml) were added to a buffer containing 130 mM KCl, 2 mM $MgSO_4$, 50 μM EGTA, and 10 mM Hepes, pH 7.2, plus 3 μM acridine orange (*AO*) in the absence (*panel A*, and *trace a* in *panel* B) or in the presence (*panel B*, *trace b*) of 10 μM AMDP. 3 μM acridine orange, 0.1 mM PP_i, 10 mM NH_4Cl, 10 μM AMDP (added in *panel A* and in *trace a* of *panel B*), and 10 mM NH_4Cl were added where indicated by the *arrows*. Control activity was $1.23 \pm 0.32 \times 10^3$ $\Delta A_{493/530}$/min/mg of protein.

sequence in the C-terminal region of the protein which is conserved in the *C. reinhardtii* sequence available in GenBank (accession numbers AV633609 and AJ304836) (Fig. 9*C*). Anti-

TABLE I
Effect of buffer composition on pyrophosphatase activity in Chlamydomonas

Rates are relative (%) to the 130 mM KCl buffer. All buffers contained, in addition, 2 mM $MgSO_4$, 10 mM Hepes, and 50 μM EGTA and were adjusted to pH 7.2 with NaOH, KOH, or Tris for NaCl, KCl salts, and sucrose buffers, respectively. Values are the means ± S.E. of the number of experiments indicated in parentheses. Control activity was 0.54 ± 0.025 μmol/min/mg of protein. Rates were corrected by subtraction of nonspecific activity in the presence of 30 μM AMDP.

Experimental conditions	Pyrophosphatase activity
	% of control
130 mM KCl	100 ± 3.8 (12)
250 mM sucrose	22 ± 11.8 (4)
130 mM NaCl	13 ± 7.2 (4)
65 mM NaCl and 125 mM sucrose	16 ± 13.1 (3)
65 mM KCl and 65 mM NaCl	58 ± 4.3 (4)
65 mM KCl and 125 mM sucrose	70 ± 13.6 (4)

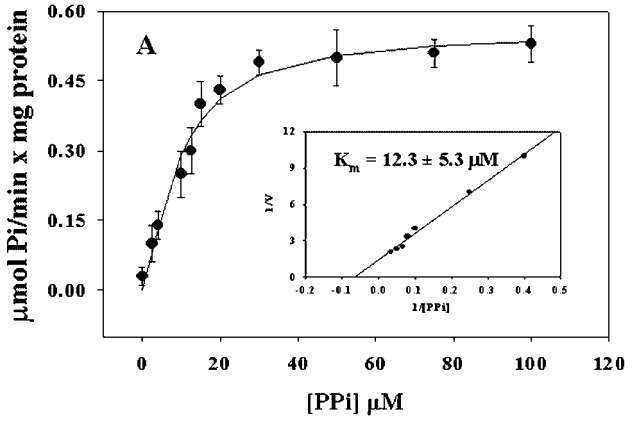

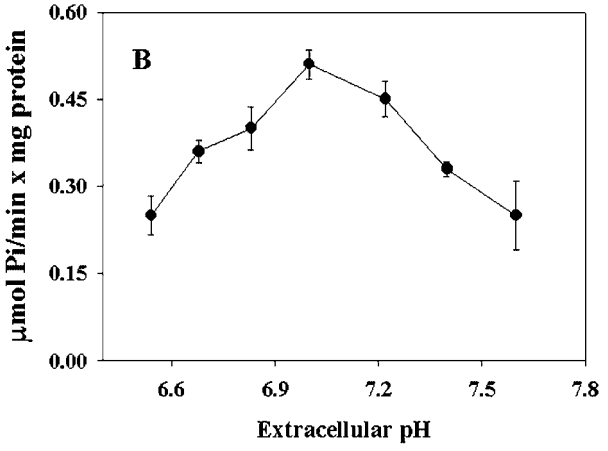

FIG. 6. **Initial rate of PP_i hydrolysis as a function of PP_i concentration (*panel A*) or medium pH (*panel B*).** Aliquots of electron-dense vacuoles, 5–10 μg of protein/ml, were added to the standard reaction mixture (Fig. 5) in the presence of increasing concentrations of PP_i or incubated in the same buffer adjusted to different pH values. *Error bars* indicate the S.E. of the means from at least four separate experiments. The *inset* in *panel A* represents the linear transformation, by double-reciprocal plot, of the curve. The K_m for PP_i was calculated by using a computerized nonlinear regression program (Sigma Plot 1.0; Jandel Scientific) to analyze the data with the Michaelis-Menten equation.

body 326 showed cross-reactivity with a band of 65 kDa present in *C. reinhardtii* (Fig. 9*B inset*, *lane PPase*). No background staining was observed when normal serum was used as a control (Fig. 9*B inset*, *lane C*). The same size of reactive polypeptide was seen in the PPase-containing fractions of iodixanol gradients (Fig. 3, *lower panel*). The reaction of these

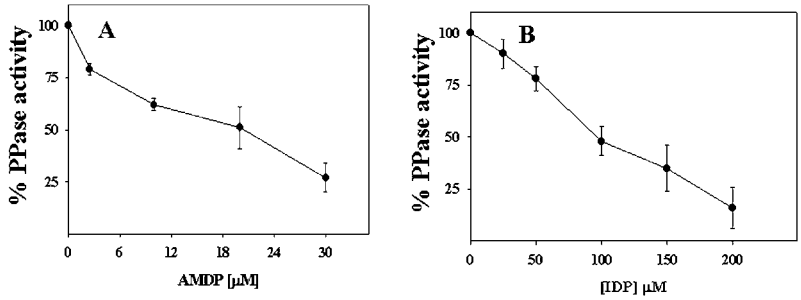

FIG. 7. **Inhibition of PP_i-dependent PP_i hydrolysis by PP_i analogs in electron-dense vacuoles.** Assays were run in the standard buffer described in Fig. 5 as indicated under "Experimental Procedures." Aliquots of electron-dense vacuoles, 5–10 μg of protein/ml, were added to the standard reaction mixture in the presence of increasing concentrations of AMDP (*A*) and IDP (*B*). The percent inhibition compared with the control in the absence of inhibitors (100%) is indicated. Control activities were 0.48 ± 0.05 μmol of PP_i consumed/min/mg of protein. *Error bars* indicate the S.E. of mean values from at least five separate experiments.

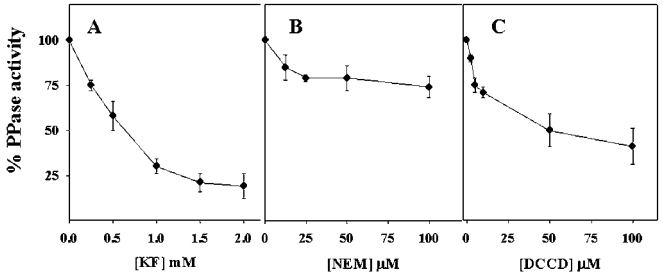

FIG. 8. **Inhibition of PP_i hydrolysis in electron-dense vacuoles by potassium fluoride, *N*-ethylmaleimide (*NEM*), and DCCD.** Assays were run in the standard buffer described in Fig. 5 as indicated under "Experimental Procedures." Aliquots of electron-dense vacuoles (5–10 μg of protein/ml) were assayed for PP_i hydrolysis in the standard reaction mixture in the presence of increasing concentrations of potassium fluoride, *N*-ethylmaleimide, and DCCD. Rates are relative (%) compared with control without inhibitor. Control activity was 0.48 ± 0.05 μmol of PP_i consumed/min/mg of protein for PP_i hydrolysis.

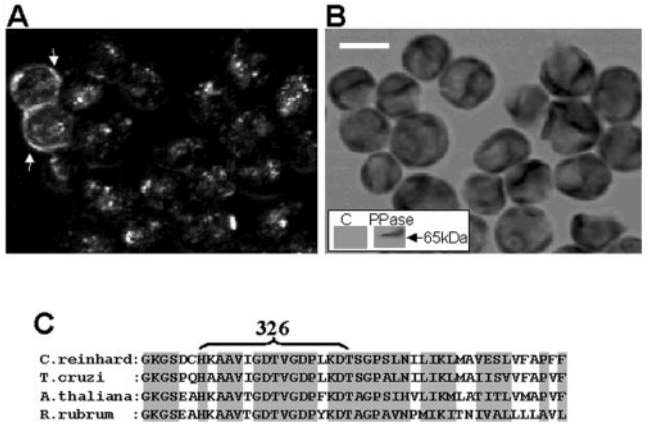

FIG. 9. **Western blot analysis and confocal immunofluorescence analysis of V-H^+-PPase in *Chlamydomonas* cells.** Fluorescent (*panel A*) and bright field (*panel B*) images of *Chlamydomonas*. *Panel A* shows intense labeling of cytoplasmic vacuoles and the plasma membrane of some cells (*arrows*) as detected using antibody 326 against the plant H^+-PPase as described under "Experimental Procedures." *Bar* (for *panels A* and *B*), 5 μm. The *inset* in *panel B* shows the detection of the H^+-PPase by immunoblot, using antibody 326, specific for the plant enzyme. 30 μg of *C. reinhardtii* proteins from the electron-dense vacuole fraction was separated by SDS-polyacrylamide gel electrophoresis and transferred to nitrocellulose. *Lane C*, immunoblot probed with normal rabbit serum. *Lane PPase* shows immunoblot probed with antibody 326. The H^+-PPase antibody recognized a polypeptide with an apparent molecular mass of 65 kDa. *Panel C*, CLUSTALW alignment of the C-terminal region of putative H^+-PPases from *C. reinhardtii* (GenBank accession numbers AV633609 and AJ304836), *T. cruzi* (AF159881), *R. rubrum* (AAC38615), and *A. thaliana* (AC005679). Identical residues are *shaded*. The *line* above the alignment shows the peptide sequence against which antibody 326 was made (13).

antibodies as revealed with fluorescein-labeled secondary antibodies was observed in small and large vacuoles, the latter corresponding to the contractile vacuole bladders (Fig. 9*A*), with a weak labeling on the cell surface of some cells (Fig. 9*A*, *arrows*). No fluorescence was observed in control parasites incubated only in the presence of the secondary fluorescein-labeled goat anti-rabbit IgG (data not shown).

Colocalization studies were done using the antibodies to the H^+-PPase (Fig. 10*A*) and a monoclonal antibody that recognizes the 110-kDa accessory protein of the V-H^+-ATPase (Fig. 10*B*) (12). This monoclonal antibody has been shown previously to cross-react with the acidocalcisomal V-H^+-ATPase of *T. cruzi* (24). Using confocal microscopy, we observed colocalization of the two proton pumps both in the contractile vacuole (Fig. 10*C*) and in smaller cytoplasmic vacuoles (areas in *yellow* in Fig. 10*C*). These results are in agreement with the colocalization of the V-H^+-ATPase and the H^+-PPase to electron-dense vacuoles and contractile vacuoles (Fig. 3). Interestingly, as occurs with *T. cruzi* acidocalcisomes (9), not all of the vacuoles show the presence of both antigens.

Evidence for Localization of Polyphosphate in the Polyphosphate Bodies and Contractile Vacuole—In addition to the subcellular fractionation results indicating cosedimentation of polyphosphate with acidocalcisomal (H^+-PPase) and contractile vacuole (V-H^+-ATPase) markers (Fig. 3) we also investigated the location of polyphosphate using DAPI (Fig. 11). DAPI is a useful tool in the fluorometric analysis of DNA but can also be used to study polyphosphates (20, 26, 27). DAPI has a fluorescence emission maximum at 456 nm. Polyphosphate shifts DAPI fluorescence to a higher wavelength with a maximum at about 525 nm (26). This DAPI fluorescence change is specific for polyphosphate and is not produced by PP_i or other anions (20, 26). *C. reinhardtii* cells incubated in solutions of DAPI (0.2 mg/ml) were mounted on slides and examined by confocal fluorescence microscopy. Using an argon laser we detected staining of numerous intracellular vacuoles that in some cells fused into large vacuoles corresponding to contractile vacuole bladders (Fig. 11). No staining was detected when DAPI was omitted (data not shown).

DISCUSSION

In this work we have identified and characterized an H^+-translocating pyrophosphatase activity in *C. reinhardtii*. Subcellular fractionation studies using iodixanol gradient centrifugation indicated that most of the H^+-PPase activity was present in the densest fractions, separate from the location of established organelle markers. Electron microscopy of the densest fractions from the iodixanol gradient showed that they contained electron-dense organelles (Fig. 4*A*) with morphology similar to that of the acidocalcisomes described in trypanoso-

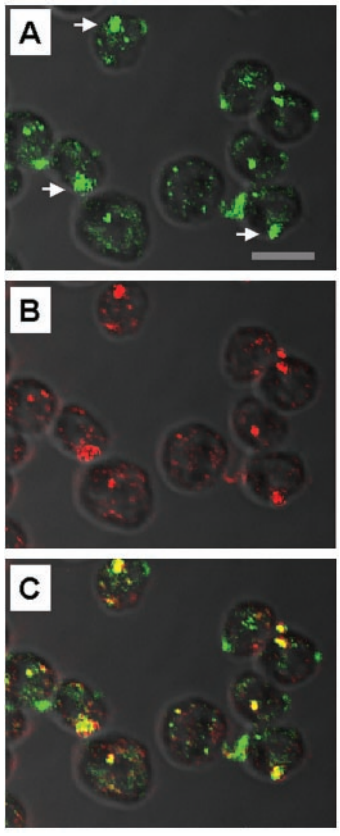

FIG. 10. **Confocal laser scanning microscopy showing the co-localization of H^+-PPase (*panels A* and *C*, in *green*) and V-H^+-ATPase (*panels B* and *C*, in *red*) in *C. reinhardtii*.** Some of the vacuoles, notably contractile vacuoles (*arrows*), labeled with both antibodies, appear in *yellow* in *panel C*. *Bar*, 10 μm.

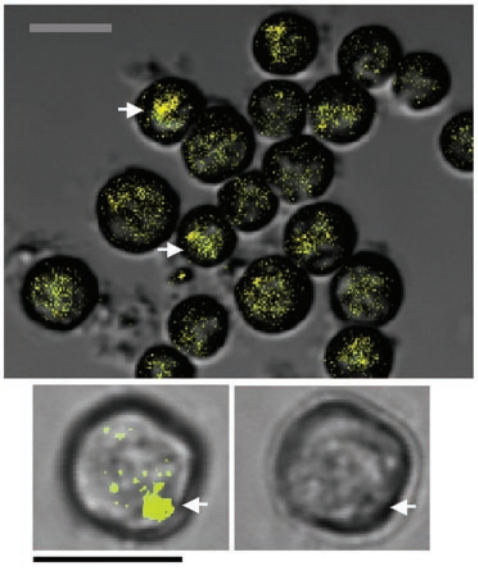

FIG. 11. **Confocal laser scanning microscopy showing the localization of polyphosphate using DAPI.** Cells were treated with DAPI as described under "Experimental Procedures." Note the accumulation of DAPI fluorescence in small vacuoles that appear to fuse into a contractile vacuole (*arrows*). The *lower panels* show a bright field image of a cell at higher magnification (*right*) and superimposition of DAPI staining of the contractile vacuole and polyphosphate bodies (*left*). *Bar*, 10 μm.

matids and apicomplexan parasites (6). As occurs with acidocalcisomes (6, 20), chemical analysis of the electron-dense vacuoles revealed the presence of large amounts of PP_i and short and long chain polyphosphate. X-ray microanalysis of these organelles yielded spectra with peaks indicating phosphorus, magnesium, calcium, and zinc (Fig. 4*B*), an elemental composition typical of acidocalcisomes (6). Acridine orange uptake by these organelles in the presence of PP_i was reversed by NH_4Cl, indicating that PP_i induced organelle acidification. The pyrophosphatase activity was optimal at pH 6.8–7.2 (Fig. 6*B*). PP_i-driven proton transport was blocked (Fig. 5), and PP_i hydrolysis was inhibited (Fig. 7) by the PP_i analog AMDP. PP_i hydrolysis was also inhibited by sodium ions (Table I), IDP (Fig. 7), potassium fluoride, *N*-ethylmaleimide, and DCCD (Fig. 8), and this activity was stimulated by potassium ions (Table I). All of these characteristics are similar to those of plant (14), trypanosomatid (15, 23), and apicomplexan (28–31) K^+-sensitive H^+-PPases. Together these results suggest that the electron-dense vacuoles or polyphosphate bodies of *Chlamydomonas* and the acidocalcisomes described in trypanosomatids and apicomplexan parasites (6) are representatives of the same class of organelle.

The polyphosphate bodies or acidocalcisomes are small organelles, with an average diameter of 200 nm (Fig. 2), and may therefore need only a few active H^+-ATPase complexes or H^+-PPases to acidify (15). It has been postulated (20) that although polyphosphates could attain molar concentrations in the acidic (pH 4–5) aqueous environment expected in the acidocalcisome, the addition of divalent cations, such as calcium and magnesium, which are present at stoichiometric concentrations in the organelles, is expected to lead to almost quantitative precipitation of the resulting complexes. Therefore it was concluded that polyphosphate in acidocalcisomes is most likely present as a microcrystalline aggregate (20), which is consistent with their very high electron density (Figs. 2*A* and 4*A*).

H^+-PPase activities have now been described in plants, bacteria, and several unicellular eukaryotes. In plants, H^+-PPases are present in the vacuole membrane (tonoplast) (7, 8) and also in the plasma membrane (32, 33). Subcellular fractionation (Fig. 3) and immunolocalization studies using antibodies to a conserved region of the plant H^+-PPase known to cross-react with the enzyme from different sources (7) (Fig. 10) revealed the localization of the enzyme in contractile vacuole bladders and in the plasma membrane of *C. reinhardtii*. A plasma membrane localization of this enzyme has been reported recently in different protozoa (23, 28, 30, 31), whereas the localization in the contractile vacuole of *Chlamydomonas* was reported before using immunoelectron microscopy (9). It had been proposed that electron-dense vacuoles of *Chlamydomonas* could fuse with the plasma membrane (34). This process could lead to the insertion of the H^+-PPase into the plasma membrane and explain the presence of antibody reactivity in only some of the *Chlamydomonas* cells if fusion was an irregular process and was followed by membrane retrieval after an interval (Fig. 9).

The contractile vacuole complex is thought to function primarily in osmoregulation, accumulating water and ions by poorly understood mechanisms and discharging their contents outside the cell by fusion with the plasma membrane (18, 19). A role for the contractile vacuole in Ca^{2+} homeostasis in *D. discoideum* has also been postulated (35). Previous reports had proposed that the V-H^+-ATPase-containing contractile vacuole bladders were related to smaller vacuoles that could fuse to form the bladders (18). However, the nature of these vacuoles was not defined. Our immunocytochemical results (Fig. 10) as well as the observation of polyphosphate by DAPI staining in vacuoles that appear to fuse into larger vacuoles (Fig. 11 and Ref. 27) suggest that polyphosphate bodies are the vacuoles that coalesce to form the contractile vacuoles. Interestingly, recent work (20) has postulated an important role in osmoreg-

ulation for the acidocalcisomes of *T. cruzi*. Polyphosphate hydrolysis occurs after hypoosmotic shock, whereas polyphosphate synthesis increases after hyperosmotic shock of the cells (20). Although there is no firm evidence of the presence of a contractile vacuole complex in *T. cruzi* several reports have postulated its presence in different trypanosomatids (36, 37), including *T. cruzi* (37), and we cannot rule out that a similar phenomenon occurs in *T. cruzi*.

Inorganic PP_i is a byproduct of several biosynthetic reactions (synthesis of nucleic acids, coenzymes, proteins, activation of fatty acids) and, in many cell types, soluble pyrophosphatases are required to hydrolyze PP_i to make these reactions thermodynamically possible. If soluble pyrophosphatases are not present in *C. reinhardtii*, the H^+-PPase may serve to degrade cytosolic PP_i, as it must do in photosynthetic plant tissues that lack soluble cytosolic pyrophosphatases (25), whereas concomitant H^+ transport may be involved in the pH regulation of the cytoplasm and intracellular compartments, as suggested in other cells (6). The colocalization of the V-H^+-ATPase and the H^+-PPase in the contractile vacuole bladders and electron-dense vacuoles of *C. reinhardtii* is analogous to what occurs with the tonoplast of plants (7, 8). The coexistence of two different enzymatic systems playing the same role in the same membrane has been postulated to be important for energy conservation (38). The H^+ gradient generated across the vacuolar membrane by the hydrolysis of either PP_i or ATP may drive both ATP and PP_i synthesis by reversal of the tonoplast H^+-ATPase (38, 39) and H^+-PPase (38), respectively.

Recent work using a polymerase chain reaction approach with degenerate oligonucleotides designed for amino acid domains common to H^+-PPases of higher plants and the photosynthetic bacterium *Rhodospirillum rubrum* allowed the identification of sequences with homology to H^+-PPases in a range of nonpathogenic trypanosomatids, in free living protozoa of other phylogenetic groups such as ciliates and heterotrophic euglenoids, and in the main phylogenetic groups of photosynthetic protists as well as in photosynthetic prokaryotes (40). Because many of these groups have been shown to possess electron-dense vacuoles or polyphosphate bodies (3), it is possible that, as in *C. reinhardtii*, this enzyme is involved in their acidification and that the phylogenetic distribution of acidocalcisomes is much wider than proposed previously.

Acknowledgments—We thank Philip A. Rea for gifts of polyclonal antibodies and AMDP, Arthur Kornberg for *E. coli* CA38 pTrcPPX1, K. Niyogi for the *C. reinhardtii* strain, John Bozzola and Steve Schmitt for help with the x-ray microanalysis, and David A. Scott for helpful suggestions.

REFERENCES

1. Meyer, A. (1904) *Bot. Zeit.* **62,** 113–152
2. Wiame, J. M. (1947) *Biochim. Biophys. Acta* **1,** 234–255
3. Kornberg, A. (1995) *J. Bacteriol.* **177,** 491–496
4. Harold, F. M. (1966) *Bacteriol. Rev.* **30,** 772–794
5. Komine, Y., Eggink, L. L., Park, H., and Hoober, J. K. (2000) *Planta* **210,** 897–905
6. Docampo, R., and Moreno, S. N. J. (2001) *Mol. Biochem. Parasitol.* **33,** 151–159
7. Drozdowicz, Y. M., and Rea, P. A. (2001) *Trends Plant Sci.* **6,** 206–211
8. Maeshima, M. (2000) *Biochim. Biophys. Acta* **1465,** 37–51
9. Robinson, D. G., Hoppenrath, M., Oberbeck, K., and Ratajczak, R. (1998) *Bot. Acta* **111,** 108–122
10. Niyogi, K. K., Björkman, O., and Grossman, A. R. (1977) *Plant Cell* **4,** 1369–1380
11. Harris, E. H. (1988) *The Chlamydomonas Source Book: A Comprehensive Guide to Biology and Laboratory Use*, pp. 25–31, Academic Press, San Diego
12. Fok, A. K., Clarke, L. M., and Allen, R. D. (1993) *J. Cell Sci.* **106,** 1103–1113
13. Zhen, R.-G., Kim, E. J., and Rea, P. A. (1997) *J. Biol. Chem.* **272,** 22340–22348
14. Zhen, R. G., Baykov, A. A., Bakuleva, N. P., and Rea, P. A. (1994) *Plant Physiol.* **104,** 153–159
15. Scott, D. A., and Docampo, R. (2000) *J. Biol. Chem.* **275,** 24215–24221
16. Kreuzberg, K., Köck, G., and Grobheiser, D. (1987) *Physiol. Plant.* **69,** 481–488
17. Klein, U., Chen, C., Gibbs, M., and Platt-Aloia, K. A. (1983) *Plant Physiol.* **72,** 481–487
18. Heuser, J., Zhu, Q., and Clarke, M. (1993) *J. Cell Biol.* **121,** 1311–1327
19. Nolta, K. V., and Steck, T. L. (1994) *J. Biol. Chem.* **269,** 2225–2233
20. Ruiz, F. A., Rodrigues, C. O., and Docampo, R. J. (2001) *J. Biol. Chem.* **276,** 26114–26121
21. Ault-Riché, D., Fraley, C. D., Tzeng, C.-M., and Kornberg, A. (1998) *J. Bacteriol.* **180,** 1841–1847
22. Leighton, F., Poole, B., Beaufay, H., Baudhin, P., Coffey, J. W., Fowler, S., and De Duve, C. (1968) *J. Cell Biol.* **37,** 482–494
23. Scott, D. A., de Souza, W., Benchimol, M., Zhong, L., Lu, H.-G., Moreno, S. N. J., and Docampo, R. (1998) *J. Biol. Chem.* **273,** 22151–22158
24. Lu, H.-G., Zhong, L., de Souza, W., Benchimol, M., Moreno, S. N. J., and Docampo, R. (1998) *Mol. Cell. Biol.* **18,** 2309–2323
25. Rea, P. A., and Poole, R. J. (1993) *Annu. Rev. Plant Physiol. Plant Mol. Biol.* **44,** 157–180
26. Allan, R. A., and Miller, J. J. (1980) *Can. J. Microbiol.* **26,** 912–920
27. Siderius, M., Musgrave, A., van den Ende, H., Koerten, H., Cambier, P., and van der Meer, P. (1996) *J. Phycol.* **32,** 402–409
28. Marchesini, N., Luo, S., Rodrigues, C. O., Moreno, S. N. J., and Docampo, R. (2000) *Biochem. J.* **347,** 243–253
29. Luo, S., Vieira, M., Graves, J., Zhong, L., and Moreno, S. N. J. (2001) *EMBO J.* **20,** 55–56
30. Rodrigues, C. O., Scott, D. A, Bailey, B. N., de Souza, W., Benchimol, M., Moreno, B., Urbina, J. A., Oldfield, E., and Moreno, S. N. J. (2000) *Biochem. J.* **349,** 737–745
31. Luo, S., Marchesini, N., Moreno, S. N. J., and Docampo, R. (1999) *FEBS Lett.* **460,** 217–220
32. Long, A. R., Williams, L. E., Nelson, S. J., and Hall, J. L. (1995) *J. Plant Physiol.* **146,** 629–638
33. Robinson, D. G., Haschke, H. P., Hinz, G., Hoh, B., Maeshima, M., and Marty, F. (1996) *Planta* **198,** 95–103
34. Komine, Y., Park, H., Wolfe, G. R., and Hoober, J. K. (1996) *J. Photochem. Photobiol.* **36,** 301–306
35. Moniakis, J., Coukell, M. B., and Janiec, A. (1999) *J. Cell Sci.* **112,** 405–414
36. Linder, J. C., and Staehelein, A. (1979) *J. Cell Biol.* **83,** 371–382
37. Clark, T. B. (1959) *J. Protozool.* **6,** 227–232
38. Rocha Façanha, A., and de Meis, L. (1998) *Plant Physiol.* **116,** 1487–1495
39. Hirata, T., Nakamura, N., Omote, H., Wada, Y., and Futai, M. (2000) *J. Biol. Chem.* **275,** 386–389
40. Perez-Catiñeira, J. R., Lopez-Marqués, R. L., Losada, M., and Serrano, A. (2001) in *New Trends in Inorganic Pyrophosphatases Research* (Serrano, A., ed), pp. 129–137, Universidad de Sevilla-CSIC, Seville, Spain